http://dx.doi.org/10.1016/j.forsciint.2015.05.010

IMPROVEMENT IN FINGERPRINT DETECTION USING TB(III)-DPICOLINATE COMPLEX DOPED NANOBEADS AND TIME RESOLVED IMAGING

Frank M. Hauser[1,2], Gerd Knupp[2] and Simon Officer*[1]

[1] School of Pharmacy and Life Sciences, Robert Gordon University, Aberdeen, Scotland
[2] Department of Applied Natural Sciences, Bonn-Rhein-Sieg University of Applied Sciences, Rheinbach, Germany

* Corresponding author: Simon Officer, School of Pharmacy and Life Sciences, Robert Gordon University, Aberdeen, Scotland, Tel: +44 (0) 1224262370; E-Mail: **s.officer@rgu.ac.uk**

Abstract

This paper deals with the synthesis and application of lanthanide complex doped nanobeads used as a luminescent fingerprint powder. Due to their special optical properties, namely a long emission lifetime, sharp emission profiles and large Stokes shifts, luminescent lanthanide complexes are useful for discriminating against signals from background emissions. This is a big advantage because latent fingerprints placed on multicoloured fluorescent surfaces are difficult to develop with conventional powders. The complex of 2,6-dipicolinic acid (DPA) and terbium ($[Tb(DPA)_3]^{3-}$) is used for this purpose. Using the Stöber process, this complex is incorporated into a silica matrix forming nanosized beads (230 – 630 nm). It is shown that the $[Tb(DPA)_3]^{3-}$ is successfully incorporated into the beads and that these beads exhibit the wanted optical properties of the complex. A phenyl functionalisation is applied to increase the lipophilicity of the beads and finally the beads are used to develop latent fingerprints. A device for time resolved imaging was built to improve the contrast between developed fingerprint and different background signals, whilst still detecting the long lasting luminescence of the complex. The developed fingerprint powder is therefore promising to develop fingerprints on multicoloured fluorescent surfaces.

Keywords: Terbium(III) dipicolinic acid complex; Silica-based nanobeads; Lanthanide luminescence; Fingerprint powder;

Introduction

The identification of individuals based on their fingerprints is very common worldwide [1]. Fingerprint powders are widely used to develop latent fingerprints encountered during an investigation on different surfaces. The purpose of fingerprint powders is to increase the contrast between fingerprint and background, however conventional powders do not show high contrast on multicoloured surfaces [2]. To develop fingerprints on such surfaces, fluorescent powders are used which utilise the visible emission of fluorescent dyes after excitation to increase the contrast between fingerprint and background [3]. If the background is also fluorescent then these powders have a limited usability and therefore luminescent fingerprint powders which are able to develop fingerprints on fluorescent surfaces are needed [4].

Lanthanides are metals which show special optical properties including sharp emission profiles, a large Stokes shift [5] and long luminescence lifetime in solution [4]. These properties are based on the principle of their luminescence. Lanthanides absorb light with a low efficiency on their own; therefore they have to be sensitised using an antenna (generally an organic chromophore as a ligand [6]) which is illustrated in Figure 1 [7]. The energy difference between the ligand and lanthanide is one reason for the large difference between excitation and emission wavelengths and therefore the Stokes shift.

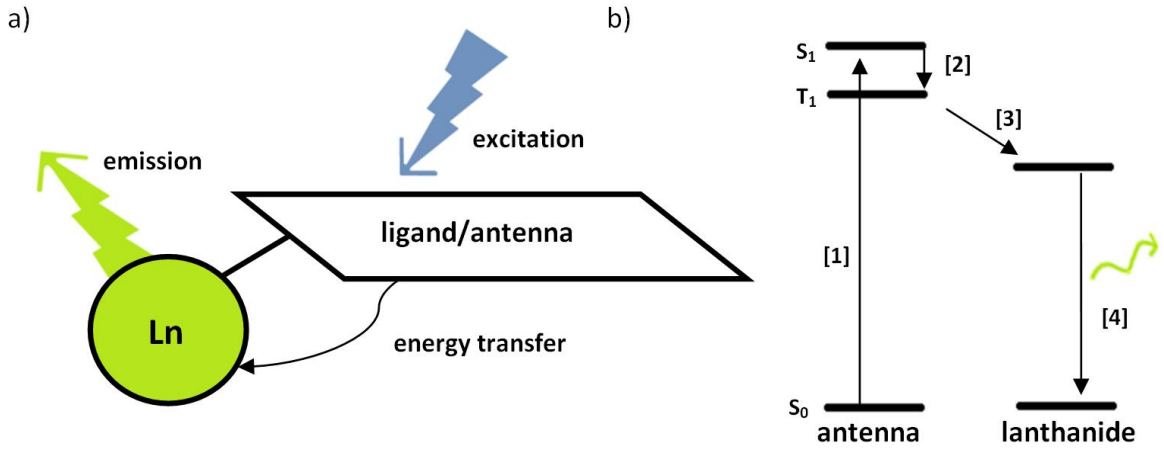

Figure 1: a) The ligand acts as an antenna and is excited by UV light. The absorbed energy is transferred to the lanthanide (Ln) which then emits light. b) An energy diagram showing the luminescence of lanthanide complexes. [1] The antenna is excited by UV-light from the S_0 to the S_1 level. [2] Via intersystem crossing the S_1 level changes to the T_1 level. [3] The T_1 level of the ligand transfers energy to the emitting state of the lanthanide. [4] The lanthanide emits light.

The mentioned properties make lanthanide complexes suitable for use in fingerprint powders to develop latent fingerprints on fluorescent surfaces. The sharp emission profile allows the filtering of interfering wavelengths leaving only the lanthanide emission, the large Stokes shift allows for separation of excitation and emission wavelengths and the long lifetime can be used to separate the lanthanide emission from any background fluorescence [4]. The process of discriminating signals by their emission lifetime is called time resolved imaging and describes the detection of the lanthanide luminescence after the background fluorescence is extinct [8]. E. R. Menzel was the first to introduce this concept of fingerprint detection [9] and since then several publications used this approach [10–13]. Quantum yield and lifetime depend on the combination of lanthanide and ligand and their particular energy levels. Research on this field has been performed by Latva et al. [14] and others [15, 16] who showed that the complex of terbium and 2,6-dipicolinic acid (DPA) has a long lifetime (around 2.2 msec) and high quantum yield (21%) [8]. The chemical structure of this complex is shown in Figure 2. Using time resolved imaging, the complex luminescence can be separated from the background fluorescence and thereby produce a clear fingerprint image [4].

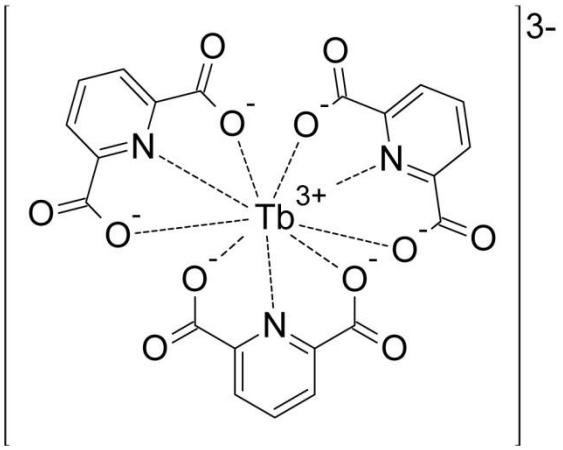

Figure 2: Chemical structure of the complex $[Tb(DPA)_3]^{3-}$

The dry complex, which forms a salt with the sum formula $Na_3[Tb(DPA)_3]\cdot 9H_2O$ [15], on its own could be used as fingerprint powder but it lacks the possibility for further optimisation. By incorporating the complex into a silica matrix, homogeneous beads with different sizes can be synthesised which also can be functionalised on the surface [6]. A simple and effective route to synthesise nanobeads (bead size up to 1000 nm [3]) is by the Stöber process [17]. This method uses the hydrolysis and condensation of a silica precursor in an alkaline alcohol solution to produce silica beads. By varying the initial parameters the particle size of the produced beads can be adjusted [18]. A small particle size is preferable for a fingerprint powder because size and also shape have an influence on the effectiveness of the powder [19] but there are also health concerns about too small beads. Due to the small size nanobeads can penetrate skin or cell membranes and cause cell death. A study by Li et al. [20] compared silica beads with different sizes from 19 to 498 nm for their effect on tumor cells. It was shown that the 498 nm beads were least toxic and that the results were comparable to the control sample. A bead size of approximately 500 nm would therefore appear to be safe and suitable for fingerprint powders since smaller particles could cause health issues and larger particles would reduce the adhesion of the powder to the fingerprint residues.

By introducing the complex $[Tb(DPA)_3]^{3-}$ into the precursor solution of the Stöber process, it is incorporated into the silica matrix [15, 21]. The surface of silica beads is hydrophilic due to SiOH groups, but the residues of fingerprints are mainly lipophilic [4]. Therefore a functionalisation of the surface can be used to increase the lipophilicity of the powder [22], which would then increase the affinity of the silica beads to the lipophilic residue of fingerprints. One method to do this has been reported by Chen et al. [23] by using phenyltriethoxysilane to introduce phenyl groups onto the surface of bentonite.

This paper reports on the synthesis of a luminescent fingerprint powder by the synthesis and subsequent incorporation of $[Tb(DPA)_3]^{3-}$ into spherical silica nanobeads by the Stöber process and investigates the effect of a lipophilic functionalisation on the properties of the beads. The use of time resolved imaging and filters is also investigated to image the developed fingerprints, remove unwanted fluorescent background emission and determine if this kind of powder should be further researched and thus improve the detection and evaluation of fingerprints in forensic practice

Materials and methods

Chemicals

All chemicals were of reagent grade and used as supplied. Ammonium hydroxide (28%) and tetraethoxy-orthosilicate (TEOS), were purchased from Sigma Aldrich. 2,6-Dipicolinic acid (DPA) was purchased from Acros Organics. Phenyltriethoxysilane (PTEOS) and terbium(III) nitrate hydrate (99.9 %) were purchased from Alfa Aesar. Nitric acid (70 %) of trace analysis grade, terbium mono-element standard for ICP (1000 mg/L) and ethanol (100 %) were purchased from Fisher. Hydranal® Composite 5 and Hydranal® methanol dry were purchased from Fluka Analytical. Granulac® 230 lactose monohydrate was purchased from Meggle. Only ultrapure water with a resistivity above 18.2 MΩ·cm was used.

Preparation of the terbium complex and the silica-based nanobeads

$Na_3[Tb(DPA)_3]\cdot 9H_2O$ complex was prepared by dissolving DPA (0.02 mol, 3.342 g) in deionised water (90 mL) containing NaOH (0.0425 mol, 1.7 g). This solution was stirred until all DPA was dissolved. Then $Tb(NO_3)_3\cdot xH_2O$ (1.815 g) was first dissolved in approximately 5 mL deionised water then added to the DPA solution and a white precipitate formed immediately. Using HCl (1 M) the pH of the solution was set to 6 and the precipitate dissolved. This solution was refluxed for two hours and the solution was evaporated until crystals began to precipitate. It was cooled down, filtered and washed with small amounts of ice cold water. The precipitate was air-dried and the yield was 4.225 g of white crystals. Purification was performed by dissolving a fraction of the white crystals (2.279 g) in a mixture of water (300 mL) and ethanol (113 mL) which was then heated to the boiling point. The solution was evaporated to a final volume of 30 mL and then ethanol was added to precipitate the complex. The precipitate was filtered and dried overnight in a desiccator. The yield of this purification step was 1.593 g and this purified complex was used for further characterisation and synthesis steps. The composition of the complex was verified by elemental analysis, infrared spectroscopy and mass spectrometry.

The silica beads were synthesised by hydrolysis of TEOS in an alkaline environment. Several batches were prepared with different starting concentrations of the complex. Table 1 shows the composition of the different starting solutions. The blank beads from batch 1 were used as a reference material. Since the complex was insoluble in ethanol, water had to be added to batches two to seven in order to get the complex into solution. An additional functionalization step was performed for batch 3. Characterization of nanobeads was performed by use of ICP-OES, particle size estimation, luminescence properties and ATR-FTIR.

Batch	$V_{ethanol}$ [mL]	V_{water} [mL]	$m_{complex}$ [mg]	V_{NH_3} [mL]	V_{TEOS} [mL]	$V_{ethanol}$ [mL]	Conc. of complex [mg/mL]
1	21.0	-	-	4	1.3	3.7	0
2	42.0	20	200	8	2.6	7.4	2.5
3*	21.0	10	100	4	1.3	3.7	2.5
4	10.5	5	40	2	0.65	1.85	2
5	10.5	5	30	2	0.65	1.85	1.5
6	10.5	5	20	2	0.65	1.85	1
7	10.5	5	5	2	0.65	1.85	0.25

Table 1: Amounts of chemicals used for different batches of the bead synthesis. The first four chemicals on the left side were mixed and a mixture of TEOS and ethanol was slowly dropped into this solution. A white precipitate was formed during this process. The resulting solution was stirred for 2 h (batches 1-3) or 3 h (batches 4-7) at room temperature, filtered and washed with water (batches 1 and 2) or ethanol (batches 4 to 7). All batches were dried using a hot water bath. * Batch 3 was, in addition, functionalised with PTEOS. After the beads were stirred for two hours a solution of 0.5 mL PTEOS mixed with 1 mL ethanol was added. The solution was stirred overnight, washed with ethanol and dried using a hot water bath the following day.

Collecting and Developing of fingerprints

Fingerprints were placed on glass slides after the hands were in gloves for several minutes to make them sweaty. The prints were dried for 5-10 minutes before they were dusted with the synthesised fingerprint powders. Because only a small amount of powder was synthesised, all of the powder was poured over the fingerprint and by tapping against the glass slide the excess powder was removed. The dusted fingerprints were excited using a handheld commercial UV lamp (UVP, model UVGL-58) at 254 nm, due to availability. Since the complex shows absorption between 250-290 nm with a peak at 270 the use of 254 nm still allowed for excitation. The results were recorded in a dark room using a reflex camera (Nikon D3200 with a 105mm Sigma macro lens). Exposure times up to 60 seconds were used to pick up the luminescence of the fingerprint powder. It has to be mentioned that UV light of 254 nm is harmful and has to be handled with care [24]. In addition 254 nm radiation causes damage to any DNA that might be present in the fingerprint [25] and will therefore eliminate the possibility to examine the fingerprints for DNA of the donor.

Instruments

Elemental analysis was carried out on a ELEMENTAR vario micro cube. Water determination was carried out using a Metrohm 870 KF Titrino plus. IR spectra of the samples in solid state were recorded on a Jasco FT/IR 410 and a Nicolet iS10 FT-IR spectrometer with an Attenuated Total Reflectance (ATR) module. MS spectra of the complex were measured with a ThermoFinnigan AQA mass spectrometer equipped with electrospray ionisation -ESI (capillary 4,00 kV, source voltage : 10 V); sample infusion was done with a Harvard Apparatus syringe pump 11 Plus. Luminescence analysis was performed using a Perkin Elmer LS 55 luminescence spectrometer. The particle sizes were estimated using a Zeiss EVO LS10 scanning electron microscope (SEM). The terbium contents of the complex

and beads were determined using a Perkin Elmer ICP with Optima 7000 DV optical emission spectrometer. A Thermo Scientific Helios Alpha UV-Vis spectrophotometer was used to collect absorption spectra.

Water determination of the terbium complex

The method for the water determination was taken from Metrohm [26]. An exact amount of approximately 60 mg complex was used for each analysis and lactose monohydrate was used as a water standard to determine the concentration of the titrant. The standard was analysed five times and the complex three times.

ICP-OES analysis

The silica beads were digested using sodium hydroxide to set free the terbium. Each batch was digested twice to perform a repeat determination. An exact amount of approximately 12.5 mg silica beads was put into a 100 mL volumetric flask. One pellet of NaOH (approximately 100 mg) and water (10 mL) were added. This suspension was heated up to the boiling point at which the solution became clear. It was boiled for one minute before it was removed from the heater. The solution was cooled to room temperature and nitric acid (3 mL, 70 %) was added. The flask was then filled with distilled water up to the 100 mL mark.

To analyse the complex for its terbium content an exact amount of approximately 30 mg complex was put into a 100 mL volumetric flask and solved in water. Out of this solution 1 mL was put into another 100 mL volumetric flask and one NaOH pellet and nitric acid (3 mL, 70 %) was added. The flask was filled with water and this solution was used for analysis.

The solutions were analyzed using an ICP-OES system. The emission at 350.917 nm was used to quantify the terbium concentration and each solution was analysed three times. An external calibration using five standards from 0.05 to 5 mg/L terbium was utilised for quantification using a terbium mono element standard (1000 mg/L) as stock solution. Batch 1 was digested and analysed as a negative control and spiked samples were used as positive controls.

LC-MS analysis

A 1 mg/mL solution of complex dissolved in water was prepared for analysis. 95% methanol and 5% water was employed as eluent and a guard column was used. Negative ionisation mode was used with 35 V as the ionisation strength and a volume of 20 µL was injected for analysis.

Lifetime determination

The emission lifetimes of $Na_3[Tb(DPA)_3]\cdot 9H_2O$ and batch 2 were determined using time-resolved luminescence. A small portion of substance was dispersed in two drops of acetone and this suspension was applied as a film on one side of a 5 mm cuvette. The film was dried and the cuvette was put into the luminescence spectrometer. The coated side of the cuvette was placed in the optical path in order to make the measurement. The measurement method was taken from Perkin Elmer [27] and a gate time of 1 msec, a cycle time of 20 msec, 5 nm

slit widths for excitation/emission and a flash count of 1 were used. UV light of 270 nm was used to excite the sample and the corresponding emission intensity at 544 nm was collected. The analysis was started with a delay time of 0.05 msec and if the intensity exceeded the detectable system range, the delay time was increased to produce a weaker signal. In the beginning the delay time was increased in 0.1 to 0.3 msec steps and the corresponding intensities were recorded. Plotting the intensities against the delay times produced a curve with an exponential decay. By calculating the natural logarithm of the intensities ln(intensity) and plotting them against the corresponding delay times a linear curve was obtained. The slope of this curve was used to calculate the lifetime according to equation 1 and the result was the lifetime of the sample in msec.

$$\tau = -1/slope \qquad [1]$$

Time resolved imaging

A reflex camera was used to take pictures of fingerprints which were dusted with the synthesised compounds. Using an optical chopper wheel to pulse the UV excitation light, time resolved photos were taken. Figure 3 shows the self build device which was used to collect time resolved photos of dusted fingerprints.

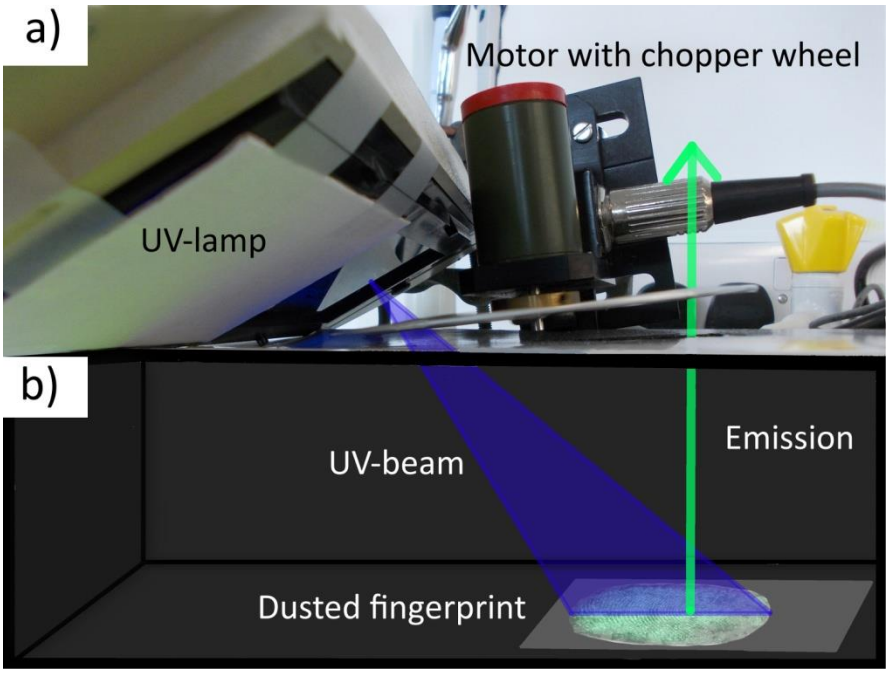

Figure 3: Device to perform time resolved imaging with dusted fingerprints inside a box. a) shows the assembly of the motor and optical chopper wheel outside the box and how the excitation and emission light pass through. b) shows the position of the fingerprint inside the box. The emission was collected using a reflex camera with 60 sec. exposure time and an ISO setting of 3200.

To build the time resolved imaging device, two holes were cut into the back of an empty glove box. A fingerprint on a glass slide was positioned directly under one of the holes. The masked UV-lamp (UVP, model UVGL-58) was placed outside at the other hole and tilted to shine on the fingerprint with a wavelength of 254 nm. An optical chopper wheel attached to a motor was positioned above both openings. One third of the wheel was open and the rest was

masked with tin foil and therefore only one hole was open at any point of time. This assembly allows the separation of excitation (hole at UV-lamp is open) and photo taking (hole above fingerprint is open). A reflex camera was placed above the fingerprint and photos were taken through the hole in a dark room. An exposure time of 60 sec was used and a high speed of the optical chopper wheel.

In addition filters were used to reduce the background fluorescence in order to compare this method with the time resolved imaging. Therefore a Comar 320 GB 50 band-pass filter for the excitation and a Comar 515 GY 50 long-pass filter for emission were used to increase the contrast. The excitation filter cuts off any wavelength longer than 400 nm whilst the emission filter removed any light below 500 nm which was produced by background luminescence.

Luminescence analysis

Emission and excitation spectra of the samples were collected using time resolved luminescence. A 5 mm cuvette was coated with the corresponding sample and placed in the luminescence spectrometer. The delay time was set to 0.05 msec, the gate time to 1 msec, the cycle time to 20 msec and the flash count to 1. If the intensity exceeded the detectable system range, the delay time was increased to produce a weaker signal. 270 nm was used as excitation wavelength to collect the emission spectra, 544 nm was used as the emission wavelength for excitation analysis, the excitation and emission slit widths were set to 8 nm and 800 nm/min was used as scan speed.

Results and discussion

Characterisation of the terbium complex

The theoretical sum formula of the synthesised complex is $Na_3[Tb(DPA)_3]\cdot 9H_2O$ and the calculated water content based on this sum formula is 17.95 %. Three repetitive analysis were performed using Carl-Fisher titration. The mean value of 18.52 % +/- 0.016 % is near to the assumed amount of crystal water and the excess water could be due to adherent water on the surface of the crystals. The elemental C,H,N-analyses values are in agreement with the expected values: found (calculated) C: 28.84 (28.49), H: 3.30 (3.07), N: 4.81 (4.75).

The theoretical terbium content of the complex was 17.9 % based on the formula $Na_3[Tb(DPA)_3]\cdot 9H_2O$. Using ICP-OES the terbium amount of the synthesised complex was determined as 16.1 % +/- 0.5 %. The lower amount of terbium in the sample can be due to impurities including unbound DPA in the sample which would lower the terbium concentration. Since the complex was purified this remaining amount of DPA should be low. In addition, adhering water on the crystals will reduce the terbium concentration of the complex.

Since crystal water is not indicated in LC-MS, the theoretical formula of the analysed complex was proposed to be $Na_3[Tb(DPA)_3]$. This molecule has a molecular weight of 723 g/mol. Since terbium consists of only one isotope it produces fragments with only one m/z

ratio. The most important signals in the -ESI mode observed are m/z = 700; 100% $\{Na_3[Tb(DPA)_3] - Na^+\}^-$, m/z = 489; 35% $\{Na_3[Tb(DPA)_3] - 3\ Na^+ - DPA^{2-}\}^-$, m/z = 338.5; 95% $\{Na_3[Tb(DPA)_3] - 2\ Na^+\}^{2-}$

The IR spectrum is identical with reported data [11]. Main wavenumbers with %-transmission in brackets are: 3412 cm^{-1} (7.6%), 1625 cm^{-1} (1.1%), 1584 cm^{-1} (4.4%), 1434 cm^{-1} (4.3%), 1391 cm^{-1} (1.7%), 1279 cm^{-1} (22.1%), 1191 cm^{-1} (32.9%), 1073 cm^{-1} (38.1%), 1022 cm^{-1}, 923 cm^{-1}.

The combination of water content, elemental analysis, terbium content, MS analysis and IR demonstrates that the complex was successfully synthesised. Figure 6 shows the emission profile of $Na_3[Tb(DPA)_3]\cdot 9H_2O$ which shows the same signals as in the literature [15, 28]. This additional information proves that the complex was successfully formed and has the expected optical behaviour and therefore the complex can now be incorporated into the silica nanobeads.

Characterisation of the silica-based nanobeads

Terbium content (ICP-OES)

In order to optimise the doping concentration of the Tb complex into the beads, the concentration of complex was altered whilst maintaining the same composition of the beads (as detailed in batches 4-7). The functionalised batch 3 was too lipophilic and therefore the used sodium hydroxide method was not able to digest it. Each batch (4-7) was synthesised two times on different days. Each of the synthesised samples was digested twice with the sodium hydroxide method and analysed using ICP-OES and therefore four samples for each concentration level were analysed. Figure 4 shows the relationship between starting amount and concentration of complex in the beads. All batches showed a similar amount of incorporated complex. Batch 1, which was used as a negative control, showed a concentration of 0.02 mg/g which indicates that there was no significant interference by the sodium hydroxide or the nitric acid used.

Based on these results it may be possible to reduce the starting concentration of complex without reducing the amount of it in the beads. All five samples showed different errors. To determine if the analytical method was responsible for this difference, a two-way ANOVA was used to determine if the replicated measurements differed significantly. This was not the case since the p-value of the replicated measurements of the first synthesis was 0.47 and the p-value of the second synthesis 0.44 (with $\alpha = 0.05$). This shows that the analytical method has a high precision and therefore it is unlikely that this was the cause of the error.

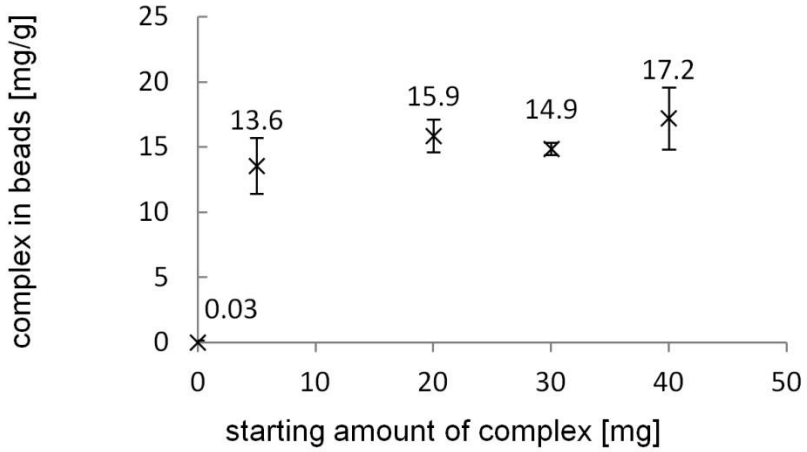

Figure 4: Concentrations of complex in batch 1 and batches 4-7. Determined using NaOH digestion and ICP-OES to determine the Tb content at 350.917 nm. The terbium content was used to count back the amount of incorporated complex ($Na_3[Tb(DPA)_3]\cdot 9H_2O$).

Particle size (SEM)

Figure 5 shows the blank beads at a magnification of 24,990 and that the used Stöber method produced very uniform beads with a size range of between 630 to 650 nm. Table 2 lists the estimated particle sizes of all seven batches. Beads of batch 2 showed a size of 450 to 500 nm which was significantly lower than the size of batch 1. One reason for this can be the added water that was necessary to solve the complex since the composition of the precursor solution has an impact on the particle size [17]. This size of around 500 nm is in the correct range as suggested in the introduction and only beads of batch 2 and 3 showed this wanted size.

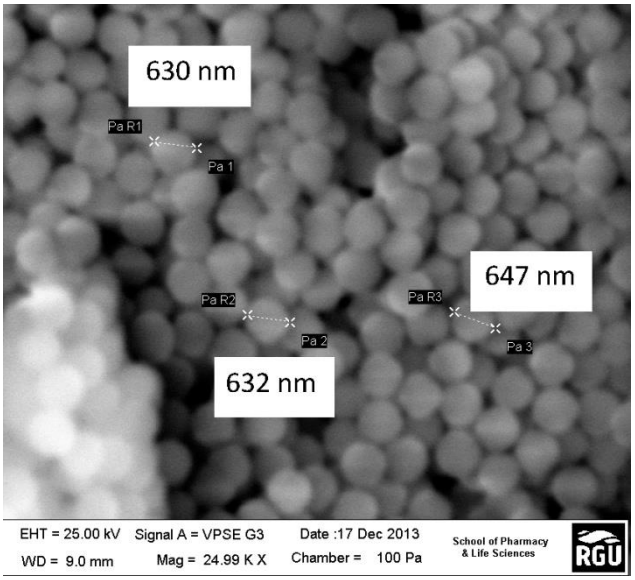

Figure 5: SEM image of beads from batch 1 at a magnification of 24.99K and a pressure of 100 Pa. The average particle size was 630-650 nm.

It can also be shown that a lower concentration of complex reduced the size of the beads which can be seen in the trend from batch 4 to 7. Therefore further research in this area has to be performed to determine the optimal reaction conditions to form the beads.

Batch	Particle size [nm]
1	630 - 650
2	450 - 500
3	480 - 500
4	360 - 390
5	350 - 360
6	290 - 310
7	230 - 260

Table 2: Particle sizes of the synthesised batches estimated using SEM.

The terbium determination using ICP-OES showed that the starting amount of the complex could be reduced without lowering the incorporated concentration. However, the SEM results indicated that this then decreased the size of the produced particles. It may be possible to synthesise particles of 500 nm in combination with a lower $Na_3[Tb(DPA)_3]\cdot 9H_2O$ amount at the beginning by adjusting the composition of the precursor solution. This may be achieved by reducing the amount of water that is used to dissolve the complex.

Luminescence spectra and lifetime determination

Figure 6 shows the emission spectra of $Na_3[Tb(DPA)_3]\cdot 9H_2O$ and batches 1, 3, 4 and 7. Batch 1 was used to show the spectrum of the blank beads, batch 3 was included since the beads were functionalised and batches 4 and 7 because they were synthesised using the same precursor solution but different starting concentrations of the complex. Batches 3, 4 and 7 showed the same emission pattern as the complex which shows that the complex was successfully incorporated into each batch without altering the spectral characteristics of the complex. The luminescence of the incorporated complex was still strong enough to be picked up with the luminescence spectrometer. The emission maxima were at 491, 544, 585 and 622 nm and $Na_3[Tb(DPA)_3]\cdot 9H_2O$ showed one additional signal at 437 nm which was very weak compared to the other signals. The strongest signal was observed at 544 nm and this wavelength was therefore used for lifetime analysis. The blank beads showed a very weak emission signal at 544 nm which was much lower than any other observed signal.

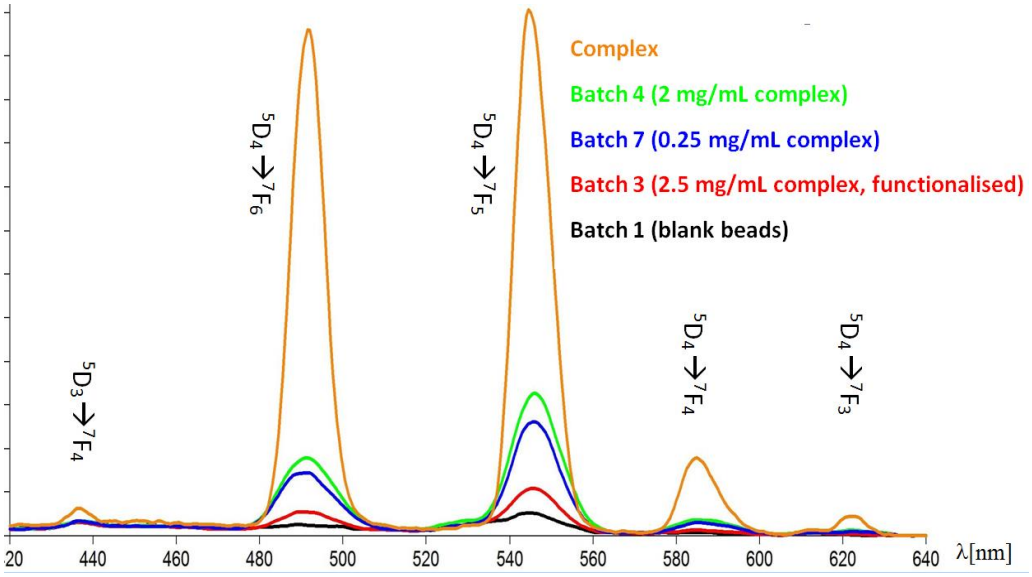

Figure 6: Emission spectra of $Na_3[Tb(DPA)_3]\cdot 9H_2O$ and batches 4, 7, 3 and 1 with an excitation wavelength of 270 nm and corresponding energy levels. A delay time of 1.5 msec for $Na_3[Tb(DPA)_3]\cdot 9H_2O$ and a delay time of 0.05 msec for the beads was used.

A visual comparison of the analysed substances under UV light showed that the pure complex had the strongest emission and that the emissions of batches 4 and 7 were weaker but still visible. The blank beads and the beads of batch 3 showed no visible green emission which indicates that there was no complex present or that the luminescence is quenched in some way. These findings are also supported by the luminescence spectra in Figure 6, which show that the pure complex had the strongest emission intensity, that batches 4 and 7 had a weaker emission intensity and that the emission intensities of batch 3 and 1 were even lower. However this is only a rough estimation since the application of the beads was not quantitative, although it was tried to apply the same amount of sample each time. Therefore differences in the application may alter the observed intensities. In addition the ICP-OES analysis showed that batches 4 and 7 had similar amounts of complex incorporated which also supports the observation that both batches show similar intensities. However further research should use a reproducible method to apply the beads for luminescence analysis in order to make quantitative conclusions.

The excitation maximum for $Na_3[Tb(DPA)_3]\cdot 9H_2O$ was determined as 270 nm. This represents the energy of the S_1 level of the ligand and therefore this wavelength was used as excitation wavelength for all luminescence experiments. The energy level diagram shown in Figure 7 was constructed using the determined emission and excitation maxima. The energy of the triplet state was taken from Latva et al. [14]. It shows that the ligand is excited to the S_1 level and then, via ISC, the ligand reaches the T_1 level. From this level the energy is transferred mainly to the $^5D_4$ level of terbium which then releases the energy in the form of the characteristic green light of Tb^{3+}. The $^5D_3$ level shows only a weak emission intensity (seen in Figure 6) due to an inefficient transfer from the close lying triplet energy level.

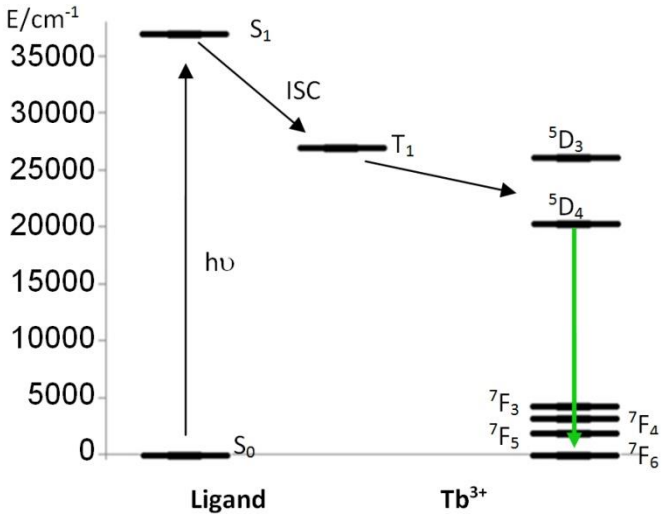

Figure 7: Energy diagram of $[Tb(DPA)_3]^{3-}$ with the corresponding singlet and triplet states. The strong green emission is due to the difference between $^5D_4$ and the different ^7F orbitals. The energy levels were calculated using the determined excitation and emission maxima and a literature value for the triplet state ($27050cm^{-1}$) [14].

Batch 3, which was coated with phenyl groups, shows the lowest intensity of the synthesised batches. The phenyl groups introduced by PTEOS absorb light of 270 nm and below and therefore reduces the UV light intensity which is needed to excite the complex inside the beads. This is likely one reason for the reduced emission intensity of batch 3 and therefore this functionalisation is of limited use in combination with the used complex. Another reason could be that there was a lower amount of $Na_3[Tb(DPA)_3]$ in batch 3 and since the terbium analysis using ICP-OES did not work this is a task for further research. Another digestion method which can digest these lipophilic beads could be used to determine the concentration of complex in them. If there was indeed a lower amount of complex present, this can also be the cause of the lower emission intensity. But since the synthesis was the same as for the other batches with the exception of one additional functionalisation step at the end, it is not expected to find a lower amount in this batch.

The emission lifetime of $Na_3[Tb(DPA)_3]\cdot 9H_2O$ was determined using the time resolved luminescence of the complex. Figure 8 shows the exponential decay of the intensities of the complex after different delay times. Since the intensity was too high at shorter delay times; the determination starts at 2 msec. The determined lifetime was 2.4 msec for the pure complex. The intensities between 2 and 5 msec were used for the calculation since the plot of ln(intensity) against the corresponding delay times was not linear anymore after 5 msec. The lifetime of batch 2 was also determined with this method and the result was 1.8 msec. This determination was started at 0.05 msec delay time and the intensity values between 0.05 and 1.5 msec were used for the calculation. Additional batches were analysed as well and showed lifetimes of 1.9 msec. This result shows that the emission lifetime is affected by the incorporation of the complex into the beads. This is proved by the same lifetime being determined in several batches which is different compared to the pure complex.

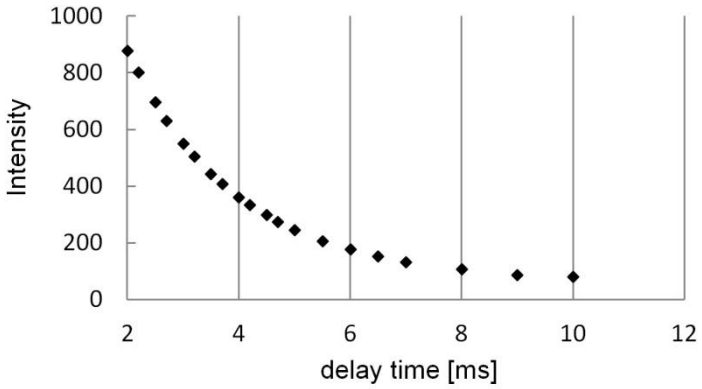

Figure 8: Lifetime determination of the synthesised $Na_3[Tb(DPA)_3]\cdot 9H_2O$ complex. The intensities at different delay times are plotted to show the exponential decay of the luminescence. 270 nm was used as excitation wavelength and 544 nm as emission.

In the beads, the complex is amorphous and therefore it has no homogeneous crystal structure. By increasing the amount of complex in the beads the lifetime may be increased which is a task for further research. The lifetime for the pure complex is similar to the research of Latva et al. [14] who determined a lifetime of 2.25 msec. The finding that the incorporated complex shows a shorter lifetime is different to the findings of An et al. [15]. In their research the lifetime of solid $Na_3[Tb(DPA)_3]\cdot 9H_2O$ was only 1.65 msec and the incorporated complex showed a longer lifetime of 1.77 msec. Their value of the incorporated complex is similar to the determined value of 1.8 msec, therefore only the lifetime of the pure complex was different. A possible explanation could be that their method to determine the lifetime results in different values. They excited their complex with 355 nm instead of 270 nm which could be the reason for the different value. Further research on this field should be performed to determine if the excitation wavelength influences the lifetime which could cause this difference.

ATR-FTIR

Figure 9 shows the ATR-FTIR spectra of the complex, the blank beads, doped beads and functionalised beads. The SiO_2 matrix produced very strong absorption bands from 1400 down to 700 cm^{-1}. This pattern is the same in the blank and doped beads. No bands of the complex were visible in the doped beads by FTIR, but since ATR only analyses the surface of the sample, it implies that the complex was successfully incorporated into the bead and was not just adhering to the surface. The functionalised beads showed additional bands at 740 and 696 cm^{-1} which was due to the aromatic phenyl groups on the surface. Both signals are strong rock vibrations of aromatic CH groups [29] which verifies that the surface was successfully functionalised with phenyl groups. The remaining spectrum shows the silica matrix. It may be possible to analyse the complex inside the beads by using Raman spectroscopy (since SiO_2 shows a weak Raman signal) or by splitting the beads open and using the ATR-FTIR again.

Based on the characterisation of the complex and the beads, it has been shown that the complex was successfully synthesised and incorporated into the silica beads. The green luminescence of the complex inside the beads was strong enough to be detectable, although the phenyl functionalisation seemed to reduce the luminescence intensity of the beads.

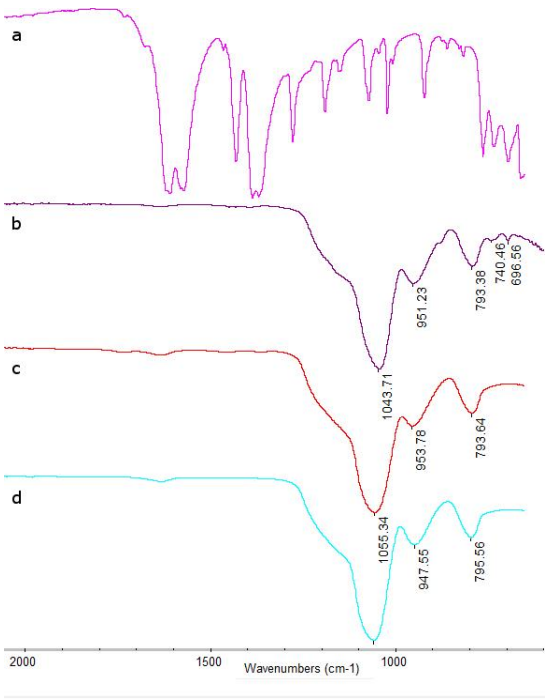

Figure 9: ATR-FTIR spectra of a) complex, b) functionalised beads (batch 3), c) doped beads (batch 2) and d) blank beads (batch 1) from 600-4000cm^{-1} with 10 repeated measurements.

Developing of fingerprints

Freshly made fingerprints were dusted with beads from all seven batches to determine if they were able to develop the latent prints. All batches were able to adhere to the latent fingerprint residues but as mentioned before only batch 2 and 3 had the desired bead size of around 500 nm and the functionalisation of batch 3 reduced the visible luminescence. Therefore only batch 2 had the anticipated properties for the use as a fingerprint powder and was used for further optimisation steps. Figure 10 shows the comparison of a freshly made fingerprint developed with the pure complex and beads of batch 2. It can be seen that batch 2 only adhered to the residue of the fingerprint whereas the complex also adhered to the background. The luminescence of the beads was weaker but the specificity for fingerprint residues was higher. By using filters the background fluorescence was reduced which increased the contrast of the fingerprint which is also shown in Figure 10.

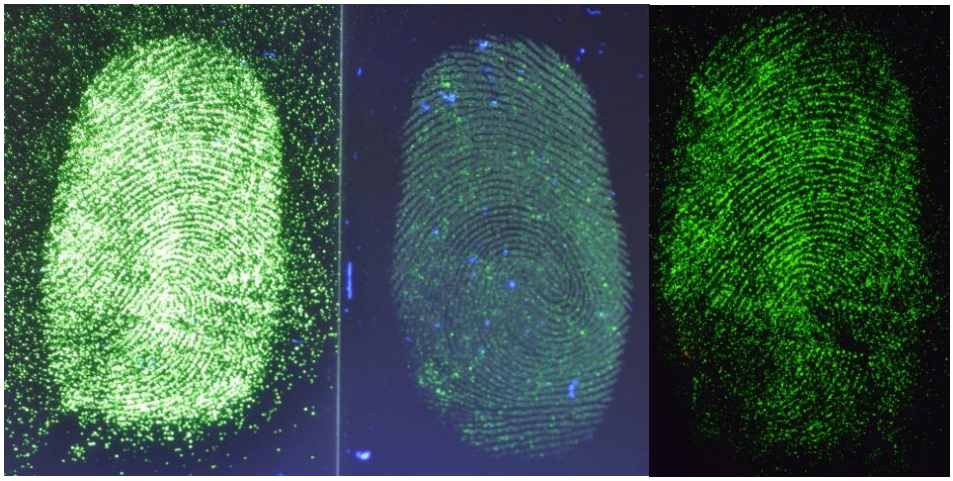

Figure 10: Comparison of fingerprints developed with $Na_3[Tb(DPA)_3]\cdot 9H_2O$ (left side) and batch 2 (middle) excited with UV light of 254 nm. The picture on the right shows the fingerprint developed with $Na_3[Tb(DPA)_3]\cdot 9H_2O$ and the use of filters to reduce background fluorescence.

Another method is to use time resolved luminescence to separate the luminescence of the powder from the fluorescence of the background. This could be useful if the filters are not enough to remove the fluorescence and it is done by using time resolved imaging. Figure 11 shows a comparison of a fingerprint dusted with $Na_3[Tb(DPA)_3]\cdot 9H_2O$ without improvement, with filters and time resolved imaging. The pure complex was used for this comparison since it showed a higher lifetime and stronger emission intensity than batch 2. A small piece of white paper and a portion of red fluorescent fingerprint powder (Crime Scene Investigation Equipment Ltd) were placed on the fingerprint to compare the print with these materials. The photo without improvement shows that the fingerprint strongly emits light but also the white paper and red dye, therefore if this fingerprint would have been placed on these materials the contrast would be low. By using filters the emission of the white paper was reduced but the red powder still fluoresced strongly. This interference of the red dye may be reduced by using an additional filter that filters emission above 560 nm, in which case only light between 500 and 560 nm would pass the filters which is the range of the strongest emission signal of $Na_3[Tb(DPA)_3]\cdot 9H_2O$. In addition a band pass filter centred at 544 nm could be used.

Only the time resolved imaging was able to cut off the background fluorescence of paper and red powder. The fingerprint luminescence became weaker but still detectable which was due to the time delay between excitation and picture taking. Picture processing was also used to reduce the blue background noise, increase the luminescence and therefore increase the contrast even more. Further research has to be performed to improve the device for time resolved imaging. Possible improvements are a shorter delay time by using a faster speed of the chopper wheel or a UV-lamp that emits light at 270 nm. This could increase the intensity of the luminescence and therefore the contrast. In addition, a time gated camera could be used that is synchronised with the chopper wheel.

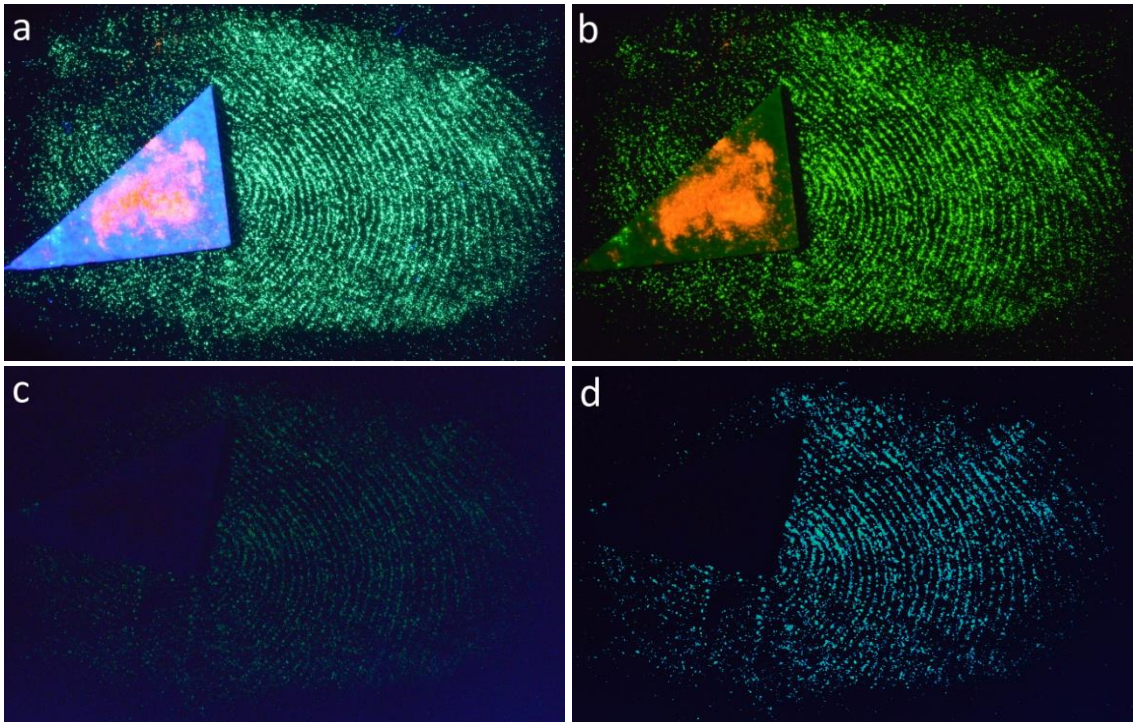

Figure 11: Comparison of a fingerprint dusted with pure $Na_3[Tb(DPA)_3]\cdot 9H_2O$ without improvement (a), with filters (b), with time resolved imaging (c) and with time resolved imaging and picture processing (d). 254 nm was used for excitation, a Comar 320 GB 50 and a Comar 515 GY filter for (b) and a self built device to take the time resolved photo for (c) and (d). Picture (d) is derived from picture (c) by reducing the brightness of the blue parts to zero and increasing colour saturation/brightness of the cyan part by 50/100.

Conclusion

The synthesis of $Na_3[Tb(DPA)_3]\cdot 9H_2O$ was successfully performed and properties of the complex were determined. This complex was successfully incorporated into silica beads using the Stöber process and the complex was detected in the beads by different methods. The emission lifetime of the incorporated $Na_3[Tb(DPA)_3]$ was shorter compared to the pure complex and further research should investigate if higher incorporated concentrations of complex could increase the lifetime of the luminescence of the beads. It was also shown that decreasing starting concentrations of $Na_3[Tb(DPA)_3]\cdot 9H_2O$ decreased the size of the produced beads but not the amount of incorporated complex. In addition, the composition of the precursor solution plays an important role and therefore further research on the ideal composition of the Stöber solution has to be performed. Furthermore, it was shown that a phenyl functionalisation on the surface of the beads reduced the luminescence and therefore an alternative functionalisation that increases the affinity of the powder to fingerprints without reducing the luminescence is needed.

The synthesised beads showed luminescence which was strong enough to develop fingerprints and be picked up by a reflex camera. Using filters the contrast of developed prints was improved by reducing background interferences. The used filters were not able to reduce the fluorescence of a red fluorescent dye and therefore a device was built which was used to take time resolved photos. This increased the contrast even more by deleting any background fluorescence and is therefore a proof of concept for the ability of this powder to be used as an

improved luminescent fingerprint powder. In a forthcoming publication we shall demonstrate additional samples from forensic practice. Further research will also be performed on this kind of powder to increase detection power and limits of the method.

Literature Cited

1. Hawthorne MR (2009) Fingerprints: Analysis and understanding. CRC Press, Boca Raton.

   http://www.worldcat.org/title/fingerprints-analysis-and-understanding/oclc/317482010&referer=brief_results

2. Sodhi GS, Kaur J (2001) Powder method for detecting latent fingerprints: a review. Forensic Science International 120: 172–176.

   http://www.ncbi.nlm.nih.gov/pubmed/11473799

3. Ramotowski RS (2013) Lee and Gaensslen's advances in fingerprint. (3rd edn), CRC Press, Boca Raton.

   http://www.worldcat.org/title/lee-and-gaensslens-advances-in-fingerprint-technology/oclc/225876335&referer=brief_results

4. Lee HC, Gaensslen RE (2001) Advances in fingerprint technology. (2nd edn), CRC Press, Boca Raton, London, New York, Washington D.C.

   http://www.worldcat.org/title/advances-in-fingerprint-technology/oclc/61503740&referer=brief_results

5. Hänninen P, Härmä H, Ala-Kleme T (2011) Lanthanide luminescence: photophysical, analytical and biological aspects. Springer, New York.

   http://www.worldcat.org/title/lanthanide-luminescence-photophysical-analytical-and-biological-aspects/oclc/745004499&referer=brief_results

6. Armelao L, Quici S, Barigelletti F, Accorsi G, Bottaro G et al. (2010) Design of luminescent lanthanide complexes: From molecules to highly efficient photo-emitting materials. Coordination Chemistry Reviews 254: 487–505.

   http://www.sciencedirect.com/science/article/pii/S0010854509002069

7. Handl HL, Gillies RJ (2005) Lanthanide-based luminescent assays for ligand-receptor interactions. Life Sciences 77: 361–371.

   http://www.ncbi.nlm.nih.gov/pubmed/15894006

8. Huang C (2010) Rare earth coordination chemistry: Fundamentals and applications. John Wiley& Sons, Singapore.

   http://www.worldcat.org/title/rare-earth-coordination-chemistry-fundamentals-and-applications/oclc/501402124&referer=brief_results

9. Menzel ER (1979) Laser Detection of Latent Fingerprints - Treatment with Phosphorescers. Journal of Forensic Sciences 24: 582–585.

   https://www.worldcat.org/title/laser-detection-of-latent-fingerprints-treatment-with-phosphorescers/oclc/4769397786&referer=brief_results

10. Campbell BM (1993) Time-resolved photography of latent prints on fluorescent backgrounds. Journal of Forensic Identification 43: 368–377.

https://www.worldcat.org/title/time-resolved-photography-of-latent-prints-on-fluorescent-backgrounds/oclc/4769352391&referer=brief_results

11. Moszczynski J, Siejca A, Ziemnicki L (2008) New System for the Acquisition of Fingerprints by Means of Time-Resolved Luminescence. Journal of Forensic Identification 58: 515–523.

http://www.theiai.org/jfi/jfi_titles.php/

12. Mitchell KE, Menzel ER (1989) Time-Resolved Luminescence Imaging: Application To Latent Fingerprint Detection. Proc. SPIE 1054: 191–195.

http://proceedings.spiedigitallibrary.org/proceeding.aspx?articleid=1256674

13. Menzel ER (1980) Fingerprint detection with lasers. M. Dekker, New York.

https://www.worldcat.org/title/fingerprint-detection-with-lasers/oclc/6223337&referer=brief_results

14. Latva M, Takalo H, Mukkala V, Matachescu C, Rodríguez-Ubis JC et al. (1997) Correlation between the lowest triplet state energy level of the ligand and lanthanide(III) luminescence quantum yield. Journal of Luminescence 75: 149–169.

http://www.sciencedirect.com/science/article/pii/S0022231397001130

15. An B, Ye J, Gong M, Yin X, Yang Y et al. (2001) Luminescence and thermal stability of sodium tris(pyridine dicarboxylate) terbate(III) complex incorporated in silica matrix by sol-gel method. Materials Research Bulletin 36: 1335–1346.

http://www.sciencedirect.com/science/article/pii/S0025540801006183

16. de Souza JM, de Sá GF, de Azevedo WM, Alves S, de Farias RF (2005) Spectroscopic study of Eu and Tb complexes on polysiloxane tridimensional networks. Optical Materials 27: 1187–1189.

http://www.sciencedirect.com/science/article/pii/S0925346704003544

17. Stöber W, Fink A, Bohn E (1968) Controlled growth of monodisperse silica spheres in the micron size range. Journal of Colloid and Interface Science 26: 62–69.

http://www.sciencedirect.com/science/article/pii/0021979768902725

18. Wang X, Shen Z, Sang T, Cheng X, Li M et al. (2010) Preparation of spherical silica particles by Stöber process with high concentration of tetra-ethyl-orthosilicate. Journal of Colloid and Interface Science 341: 23–29.

http://www.ncbi.nlm.nih.gov/pubmed/19819463

19. Wilshire B (1996) Advances in fingerprint detection. Endeavour 20: 12–15.

http://www.sciencedirect.com/science/article/pii/0160932796100053

20. Li Y, Sun L, Jin M, Du Z, Liu X et al. (2011) Size-dependent cytotoxicity of amorphous silica nanoparticles in human hepatoma HepG2 cells. Toxicology in Vitro 25: 1343–1352.

http://www.ncbi.nlm.nih.gov/pubmed/21575712

21. Magyar AP, Silversmith AJ, Brewer KS, Boye DM (2004) Fluorescence enhancement by chelation of Eu^{3+} and Tb^{3+} ions in sol–gels. Journal of Luminescence 108: 49–53.

http://www.sciencedirect.com/science/article/pii/S0022231304000109

22. Wu Z, Xiang H, Kim T, Chun M, Lee K (2006) Surface properties of submicrometer silica spheres modified with aminopropyltriethoxysilane and phenyltriethoxysilane. Journal of Colloid and Interface Science 304: 119–124.

http://www.ncbi.nlm.nih.gov/pubmed/16989845

23. Chen Q, Kerk WT, Soutar AM, Zeng XT (2009) Application of dye intercalated bentonite for developing latent fingerprints. Applied Clay Science 44: 156–160.

http://www.sciencedirect.com/science/article/pii/S0169131709000258

24. Environmental Health & Safety Office. Ultraviolet Lamp Safety Factsheet, https://www.ehs.uci.edu/programs/radiation/UV%20Lamp%20Safety%20Factsheet.pdf, accessed 06.04.2015.

25. El-Yazbi AF, Loppnow GR (2014) Detecting UV-induced nucleic-acid damage. TrAC Trends in Analytical Chemistry 61: 83–91.

http://www.sciencedirect.com/science/article/pii/S016599361400137X

26. Metrohm. KF Application Note K-52: Determination of the water content in sodium acetate with MATi 10, http://www.metrohm.co.uk/Applications/MethodsNew.html?identifier=AN-K-052&language=en&name=AN-K-052, accessed 08.04.2014.

27. Padera F. Fluorescence Application Note: Calculating Phosphorescence Lifetimes with the Perkin Elmer Model LS-50B, http://perkinelmer.co.kr/files/Calculating%20Phosphorescence%20Lifetimes.pdf, accessed 08.04.2014.

28. Xiao H, Chen M, Mei C, Yin H, Zhang X et al. (2011) Eu(III), Tb(III) complexes with novel ligands containing pyridine-2,6-dicarboxylic acid unit: Synthesis, characterization, fluorescence properties and application in biological imaging. Spectrochimica Acta Part A: Molecular and Biomolecular Spectroscopy 84: 238–242.

http://www.ncbi.nlm.nih.gov/pubmed/21993259

29. Li YS, Wang Y, Ceesay S (2009) Vibrational spectra of phenyltriethoxysilane, phenyltrimethoxysilane and their sol–gels. Spectrochimica Acta Part A: Molecular and Biomolecular Spectroscopy 71: 1819–1824.

http://www.ncbi.nlm.nih.gov/pubmed/18722154

Acknowledgements

We would like to thank the Robert Gordon University for funding and supporting this research, and also to the Bonn-Rhein-Sieg University of Applied Sciences for analysing the samples for NMR, MS, elemental analysis and IR.